

# Rainfall rate and rain attenuation contour maps for preliminary “Simon Bolivar” satellite links planning in Venezuela

Angel Dario Pinto-Mangones <sup>a</sup>, Nelson Alexander Pérez-García <sup>b</sup>, Juan Manuel Torres-Tovio <sup>a</sup>, Eduardo José Ramírez <sup>c</sup>, Samir Oswaldo Castaño-Rivera <sup>d</sup>, Jaime Velez-Zapata <sup>e</sup>, John Dwiht Ferreira-Rodríguez <sup>f</sup> & Leidy Marian Rujano-Molina <sup>c</sup>

<sup>a</sup> Escuela de Ingeniería de Sistemas, Universidad del Sinú, Montería, Colombia. angelpinto@unisinu.edu.co, juantorrest@unisinu.edu.co

<sup>b</sup> Escuela de Ingeniería Eléctrica, Universidad de Los Andes, Mérida, Venezuela. perezn@ula.ve

<sup>c</sup> Postgrado en Telecomunicaciones, Universidad de Los Andes, Mérida, Venezuela. edramirez952@gmail.com, lmarian89@hotmail.com

<sup>d</sup> Departamento de Ingeniería de Sistemas y Telecomunicaciones, Universidad de Córdoba, Montería, Colombia. sacastano@correo.unicordoba.edu.co

<sup>e</sup> Departamento de Ciencias de la Computación y Electrónica, Universidad de la Costa, Barranquilla, Colombia. jvelez@cuc.edu.co

<sup>f</sup> Departamento de Física, Universidad de Los Andes, Mérida, Venezuela. fjohn@ula.ve

Received: July 28<sup>th</sup>, 2018. Received in revised form: February 4<sup>th</sup>, 2019. Accepted: February 25<sup>th</sup>, 2019.

## Abstract

Predicting precipitation rate and rainfall attenuation are key aspects in planning and dimensioning of wireless communication systems operating at frequencies above 10 GHz, such as satellite communication systems at Ku and Ka-bands. In this paper, contour maps of rainfall rate and rain attenuation are developed for the first time in Venezuela. It is based on 1-min rain rate statistics obtained from measurements carried out in Venezuela over a 30 years period with a higher integration time. The Rice-Holmberg model, refined Moupouma-Martin model and Recommendation ITU-R P.837-7 for rain rate estimation were used, while Recommendation ITU-R P.618-13, Ramachandran-Kumar model, Yeo-Lee-Ong model and Rakshit-Adhikari-Maitra model were used for rain attenuation prediction in “Simón Bolívar” satellite links in Venezuela. The results of both types of maps represent a useful tool for preliminary planning of those links in the country, specifically, in Ku and Ka-bands.

**Keywords:** contour maps; rain rate prediction; integration-time conversion; rain attenuation estimation; satellite links.

# Mapas de contorno de tasa de precipitación y atenuación por lluvias para planificación preliminar de enlaces del satélite “Simón Bolívar” en Venezuela

## Resumen

La tasa de precipitación y atenuación por lluvias son aspectos claves en la planificación y dimensionamiento de sistemas inalámbricos de comunicaciones que operan en frecuencias superiores a 10 GHz, por ejemplo, sistemas de comunicación vía satélite en las bandas Ku y Ka. En este artículo, se desarrollan por primera vez en Venezuela mapas de contorno de tasa de precipitación y atenuación por lluvias, en base a estadísticas de lluvia de 1-minuto obtenidas a partir de mediciones realizadas en Venezuela en un periodo de 30 años con alto tiempo de integración. Se usaron los modelos Rice-Holmberg, Moupouma-Martin refinado y Recomendación ITU-R P.837-7, para estimar la precipitación, y los modelos Recomendación ITU-R P.618-13, Ramachandran-Kumar, Yeo-Lee-Ong y Rakshit-Adhikari-Maitra, para predecir la atenuación por lluvias para enlaces del satélite “Simón Bolívar” en Venezuela. Los resultados de ambos tipos de mapas representan una herramienta útil para la planificación preliminar de dichos enlaces en el país, específicamente en las bandas Ku y Ka.

**Palabras clave:** mapas de contorno; predicción de tasa de precipitación; conversión de tiempos de integración; estimación de atenuación por lluvias; enlaces satelitales.

**How to cite:** Pinto-Mangones, D, Pérez-García, N.A, Torres-Tovio, J.M, Ramírez E.J, Castaño-Rivera S.O, Velez-Zapata, J, Ferreira-Rodríguez, J.D. and Rujano-Molina L.M. Rainfall rate and rain attenuation contour maps for preliminary “Simon Bolívar” satellite links planning in Venezuela. DYNA, 86(209), pp. 30-39, April - June, 2019.



## 1. Introduction

In 2008, Venezuela launched its first satellite, “Simón Bolívar”, into space. It is a telecommunications satellite located in the geostationary orbit at 78° W longitude and operates at C, Ku and Ka-bands [1]; hence, it is necessary to consider the impact of rain events on satellite links performance, which deteriorates the carrier-to-noise ratio (C/N) in the uplink and downlink, to the point that the system may become unavailable in case of being undersized or involved in an investment higher than necessary, if the system is oversized [1].

Rain affects telecommunication systems operating in frequencies above 10 GHz. At these frequencies, raindrop sizes have similar magnitude that signal wavelength, and one part of the electromagnetic wave energy is absorbed and dispersed, resulting in attenuation at the received power [1]. If these effects are not properly estimated, it may result in undersized/oversized links.

Previous studies have shown several models rain attenuation prediction for satellite communication systems, for example, Recommendation ITU-R P.618-13 [2], Ramachandran-Kumar model [3], Yeo-Lee-Ong model [4] and Rakshit-Adhikari-Maitra model [5]. These models depend on rain rate,  $R$ , so accuracy in predicting rain attenuation is mainly related to whether or not rain measurements exist in the locality of interest. Here, it is important to emphasize that the rain rate cumulative distribution to be used in rain attenuation models should be constructed from measurements performed with very short temporal resolution, i.e., 1-min integration time or less [1,6,7]. This means that in countries, like Venezuela, where such statistics are not available, it is necessary to implement conversion methodologies (e.g., Recommendation ITU-R P.837-7 Annex 2 [6]) or analytical formulations (e.g., Rice-Holmberg model [8], refined Moupouma-Martin model [9] and Recommendation ITU-R P.837-7 Annex 1 [6]) to obtain cumulative distributions of precipitation rate suitable for satellite links planning, from statistics with longer integration times (e.g., hourly, daily and monthly), considering local climate information.

This study continues the research initiated by Rujano-Molina et al. [10]. It develops, for the first time in Venezuela, contour maps of rain rate for various exceedance probabilities of time,  $p\%$ , based on 1-min rainfall rate statistics at several locations of the country. These were obtained through Rice-Holmberg model, refined Moupouma-Martin model and Recommendation ITU-R P.837-7 Annex 1. In addition, rain attenuation contour maps are also generated by the widely recognized and accepted ITU model (Recommendation ITU-R P.618-13), as well as by some models developed for tropical climates, i.e., Ramachandran-Kumar model, Yeo-Lee-Ong model and Rakshit-Adhikari-Maitra model. Both maps were created and based on local rain rate and rain attenuation estimated by these models. The interpolation spatial method known as Spline [11] was used because it offers good results for less uniformly distributed data, such as those for Venezuela.

It is important to point out this work, with or without contour maps, follows other similar studies developed in other countries, for example, Colombia [12], Nigeria [13],

South Africa [14], India [15], Bangladesh [16], Brazil [17], and Libya [18], among others.

## 2. Rainfall rate conversion models

In Rice-Holmberg (RH) model, data related with short-term precipitations was extrapolated to generate rain rate cumulative distributions based on measurements made at the meteorological stations. The probability for a rain rate,  $R$ , with a 1-min integration time is mainly based on average cumulative precipitation over an annual period,  $M$ , the highest monthly precipitation in the period,  $M_m$ , and average number of days,  $U$ , with storm or convective rains within the same year [8]. The complementary cumulative distribution function (CCDF) of the rain rate,  $P(r \geq R)$ , is given by

$$P(r \geq R) = \frac{M}{87.66} [0.03\beta^{-0.03R} + 0.2(1-\beta)(e^{-0.258R} + 1.86 e^{-1.63R})] \quad (1)$$

$$\beta = (0.03 + 0.97 e^{-5e^{-0.004M_m}})[0.25 + 2e^{-0.35(1+0.125M)/U}] \quad (2)$$

It is worth highlighting that the RH model makes a good estimate of the rain rate distribution for percentages of link unavailability ( $p\%$ ), from 0.01% to 0.1% [1,12,19]. Additionally, the RH model allows to estimate rain rate cumulative distribution from measurements with high integration times (e.g. a week, month, etc.) [12,19].

Since the implementation of RH model requires the knowledge of data that is not always available from the meteorological services of a country, such as that related with convective rains, refined Moupouma-Martin (RMM) model [9,14] can be implemented. This model is used for both tropical and subtropical regions and approximates low rain rates to a log-normal distribution, while high rainfall rate is approximated by gamma distribution. The CCDF of 1-min rain rate in RMM model is defined by [1,9,14]

$$P(r \geq R) = 10^{-2} \left( \frac{R_{0,01} + 1}{R + 1} \right)^b e^{[u(R_{0,01} - R)]} \quad (3)$$

$$b = \left( \frac{R}{R_{0,01}} - 1 \right) \ln \left( 1 + \frac{R}{R_{0,01}} \right) \quad (4)$$

$$u = \frac{4 \ln 10}{R_{0,01}} e^{-[\lambda \left( \frac{R}{R_{0,01}} \right)^\gamma]} \quad (5)$$

where  $\lambda$  and  $\gamma$  are factors that depend on the climate zone. For example, for tropical and subtropical climates  $\lambda = 1.066$  and  $\gamma = 0.214$  [9].

Eq. (3)-(5), show that the rainfall rate probability,  $P(r \geq R)$ , in refined Moupouma-Martin model also depends on rain rate,  $R_{0,01}$ , exceeded at 0.01% of time in an average year. This can be estimated using the Chebil-Rahman model [20], based on a power law for rain rate calculation with a 1-min integration time by using only annual cumulative average precipitation  $M$ , in conjunction with regression parameters,  $\alpha$  and  $\beta$ , as follows

$$R_{0,01} = \alpha M^\beta \quad (6)$$

where  $\alpha$  and  $\beta$  are regression parameters equals to 12.2903 and 0.2973, respectively.

Finally, Recommendation ITU-R P.837-7 Annex 1 [6] is a global rain prediction method that considers the impact of monthly predictions of rainfall rate cumulative distribution. Input data involves the geographic coordinates (latitude, longitude) of the specific site, monthly rain rate in an annual period, time percentage of interest and monthly ground temperatures (referred 2 meters above the surface). If temperatures are not available, bi-linear interpolation from digital maps with long-term reliable data provided by [21] can be used. The Recommendation ITU-R P.837-7 Annex 1 is based on the following two assumptions [7]: a) the monthly rainfall rate statistics are approximated by log-normal distribution, whose scale parameter,  $\sigma_i$ , does not depend on the locality and is equal to 1.26; b) the monthly mean rain rate,  $r_i$ , is a function of the monthly mean ground temperature,  $T_i$ . The annual rainfall rate probability of exceedance is obtained by [6,7]

$$P(r \geq R) = \frac{\sum_{i=1}^{12} N_i P_i(r > R)}{365,25} \quad (7)$$

where  $N_i$  represents the number of days in each month.

In Eq. (7),  $P_i(r \geq R)$  corresponds to the monthly CCDF of rain rate for the  $i$ th month, defined as

$$P_i(r > R) = P_{0i} Q\left(\frac{\ln R + \frac{\sigma_i^2}{2} - \ln r_i}{\sigma_i}\right) = \frac{P_{0i}}{2} erfc\left(\frac{\ln R + \frac{\sigma_i^2}{2} - \ln r_i}{\sqrt{2}\sigma_i}\right) \quad (8)$$

$$r_i = \begin{cases} 0.5874, & \text{for } T_i < 0^\circ \text{ C} \\ 0.5874 e^{0.0883}, & \text{Otherwise} \end{cases} \quad (9)$$

where  $Q$  and  $erfc$  are the well-known  $Q$ -function and complementary error function, respectively.

In Eq. (8),  $P_{0i}$  represents the monthly probability of rain, given by

$$P_{0i} = \frac{MT_i}{24 N_i r_i} \quad (10)$$

where  $MT_i$  is monthly mean total rainfall. If  $P_{0i}$  is greater than 70, then  $P_{0i} = 70$  and  $r_i$  is calculated by

$$r_i = \frac{100}{70} \frac{MT_i}{24 N_i} \quad (11)$$

Eq. (10), shows that, if reliable long-term local data is not available,  $MT_i$  at the desired location can be determined performing a bi-linear interpolation from digital maps of mean monthly value of rainfall, provided as an integral part of Recommendation ITU-R P.837-7.

### 3. Rain attenuation prediction models in satellite links

Recommendation ITU-R P.618-13 [2] shows a method to predict rain attenuation in satellite links considering some of the following input data: operating frequency,  $f$ , effective radius of the Earth,  $R_E$ , mean elevation above sea level of the earth station,  $h_s$ , earth station elevation angle,  $\theta$ , earth station

latitude,  $\varphi$ , and rain rate to 0.01% of the time in an average year,  $R_{0.01}$ . The method estimates rain for any percentage of time ( $p\%$ ) and consists of ten (10) steps that include, among others, calculation of  $h_R$  (i.e., average annual rainfall height above the mean sea level), inclined path,  $L_s$  (depends on  $h_s$ ,  $h_R$ ,  $R_E$  and  $\theta$ ) and horizontal projection of the inclined path,  $L_G$  (depends on  $L_s$  and  $\theta$ ). The algorithm of the Recommendation ITUR P.618-13 also includes specific rain attenuation calculation for 0.01% of the time,  $\gamma_{0.01}$ , horizontal reduction factor determined for 0.01% of the time,  $r_{0.01}$  and adjustment factor in the vertical direction for 0.01% of the time,  $v_{0.01}$ . Finally, rain attenuation,  $A_p$ , exceeded during percentages of time,  $p\%$ , other than 0.01%, from 0.001% to 5% range, is calculated through interpolation in function of  $p$ ,  $A_{0.01}$  (attenuation exceeded for 0.01% of the time), earth station elevation angle,  $\theta$ , and earth station latitude,  $\varphi$ .

Ramachandran-Kumar (RK) model was developed on rain attenuation measurements performed on Ku-band satellite in Fiji, a tropical region [3]. The model considers the existence of a breakpoint, related to a change in rain structure, in the decrease of complementary cumulative distribution (CCD) of precipitation rate and shows two adjusted expressions of Recommendation ITU-R P.618-8 (published in 2003): one for lower rainfall rates at the breakpoint and another one for higher rainfall rates. According to the model, rain rate breakpoint takes place in a exceedance probability of time,  $p_R$ , approximately equal to 0.01%, while for attenuation, the percentage of time,  $p_A$ , in which the breakpoint occurs, is 2.14 times higher than  $p_R$ . Therefore, the attenuation,  $A_{0.01}$ , of original ITU-R model, becomes  $A_B$ , that is the attenuation exceeded for 0.021% of time, calculated by the original version. In general, rainfall attenuation given by RK model includes an expression for ( $0.021 \leq p < 1$ ) that incorporates a correction factor,  $C_f$ , for link elevation angle,  $\theta$ , between  $40^\circ$  and  $60^\circ$  (consider crossed slant path with more than one cell), and another expression used to estimate rain attenuation for  $p \leq 0.021$ .

Yeo-Lee-Ong (YLO) model [4] was developed on measurements carried out in six tropical countries (Thailand, Indonesia, Malaysia, Singapore, Papua New Guinea and Brazil). The method is similar to that of Recommendation ITU-R P.618-11 (published in 2013), with the following variants: a) use of a single path adjustment factor instead of the horizontal and vertical adjustment factors; this factor depends on  $\theta$ ,  $R_{0.01}$ ,  $f$ ,  $h_s$  and rain height  $H = h_R$ ; b) the regression parameters, including factor  $\beta$ , from the exponent in the interpolation expression to calculate the attenuation in original ITU-R model, are readjusted on the measurements of the six tropical regions mentioned above.

Finally, Rakshit, Adhikari and Maitra (RAM) [5] developed a model for rainfall decay parameter  $\Gamma$ , of Simple Attenuation Model (SAM) [22], using rain attenuation measurements carried out on Ku-band satellite in Calcutta, India, a tropical climate region. By applying the numerical method known as bisection, the model offers values of the aforementioned parameter depending on point rain rate,  $R_p$ , for the percentage of the time,  $p$ , in span window of 2 mm/h. In the model, rain decay parameter decreases to 25 mm/h, does not change significantly between 25 mm/h and 40 mm/h, and increases at the 40 mm/h interval.

The procedure for calculating the rainfall attenuation for a 1-minute integration time in each of the aforementioned models is shown in Appendix.

#### 4. Rain rate contour maps in Venezuela using local climatological data

Venezuela is located in the inter-tropical zone from  $0^{\circ}$  to  $13^{\circ}$  latitude North and  $59^{\circ}$  to  $54^{\circ}$  longitude West. This country has an interesting variety of climates, namely, tropical rainforest, tropical savanna, tundra, desert, steppes, and so on. In this work, monthly precipitation rate measurements made along 30 years in 35 of the Venezuela's meteorological stations is used for generating rain rate contour maps of the country to generate rain rate contour maps of the country. The measurements were supplied by the *Instituto Nacional de Meteorología e Hidrología* (INAMEH) [23] and initially explored by Rujano-Molina et al. [10]. Table 1 summarizes the information about the stations.

Table 2 shows rain rates converted to 1-min integration time for exceedance probability 0.01% (input parameter considered in various rain attenuation models) and 0.5% (a typical percentage in planning of satellite communication operating at frequencies above 10 GHz), using RH and RMM models and Recommendation ITU-R P.837-7 Annex 1.

Contour maps were constructed using the Spline method in the ArcGIS software [24] to interpolate in space the rain rate obtained through the aforementioned models. Figs. 1 and 2 show the results obtained when the RMM model was applied for both percentages of link unavailability, 0.01% and 0.5%, respectively.

As shown, for both exceedance probabilities the highest rain rates occur at southern sector (Amazon state), northeastern zone (Monagas state), western area (Táchira state, Córdoba municipality) and the most northwestern region of the country (Zulia state, Catatumbo municipality). These rates are expected because these areas correspond to regions of the country with tropical rainforest climate (i.e., Amazon), tropical savanna climate (i.e., Monagas and Tachira) and a high number of thunderstorms in an average year (i.e., Catatumbo). The lowest rain rates, on the other hand, occur at northwestern region (Falcón state) and Margarita Island, having both regions tropical desert climate. Figs. 1 and 2 and Table 1, also show that for the percentage of time equal to 0.5% the values of the precipitation rate obtained are lower than the values of such rate for 0.01% of the time. This is consistent with the well-known fact that high rainfall intensities correspond to short-duration time intervals, i.e., lower percentages of time for which rain is exceeded [1].

Table 1.  
Precipitation Data in Venezuela.

No.	Station	State	Latitude ( $^{\circ}$ )	Longitude ( $^{\circ}$ )	Altitude (m)	$M$ (mm/h)	$M_m$ (mm/h)	$U$
1	Tama-Tama	Amazonas	3.1	-65.9	225	3458.6	1052.2	70
2	San Fernando	Amazonas	4.0	-67.7	112	3020.3	699.7	70
3	La Corcovada	Anzoátegui	10.1	-64.6	98	1202.7	488.0	40
4	San Fernando de Apure	Apure	7.9	-67.5	52	1393.2	516.0	55
5	Estación Camatagua	Aragua	9.8	-67.0	328	1107.1	380.1	40
6	Barinas	Barinas	8.6	-70.2	189	1519.5	486.0	55
7	La Vitera	Bolívar	7.3	-65.8	90	1546.3	636.2	60
8	Maripa	Bolívar	7.4	-65.2	30	2027.8	587.7	55
9	Valencia-SL	Carabobo	10.1	-68.1	487	1142.1	358.1	60
10	Morita-Caserío	Cojedes	9.7	-68.2	145	1331.9	662.7	60
11	Curiapo	Delta Amacuro	8.6	-61.0	6	1795.0	397.1	50
12	Observatorio Cagigal	Distrito Capital	10.5	-66.9	967	863.7	354.9	60
13	Coro	Falcón	11.4	-69.7	22	368.8	296.0	30
14	Biol. Los Llanos	Guárico	8.9	-67.4	90	1395.7	432.8	55
15	Agua Negra	Lara	9.8	-69.5	1560	1000.5	429.6	55
16	Moroturo	Lara	10.6	-69.2	190	1087.5	394.0	55
17	El Vigía	Mérida	8.6	-71.7	100	1816.0	397.8	70
18	La Mitíus	Mérida	8.9	-70.7	1632	1416.6	400.2	65
19	Caucagua	Miranda	10.3	-66.4	69	2057.1	945.5	55
20	La Veraniega	Miranda	10.1	-66.8	170	1116.8	390.4	55
21	Tierra Blanca	Monagas	10.2	-63.6	920	1429.4	491.4	45
22	Caripito	Monagas	10.1	-63.1	36	2201.3	670.7	45
23	Tacarigua	Nueva Esparta	11.1	-63.9	46	741.3	777.4	20
24	San Juan Bautista	Nueva Esparta	11.0	-63.9	78	635.3	271.4	20
25	Guanare	Portuguesa	9.0	-69.8	166	1664.9	519.0	55
26	Cancumare	Sucre	10.3	-64.2	93	1514.7	805.2	40
27	Cariaco-Muelle	Sucre	10.8	-63.7	19	1475.3	455.1	40
28	Puente Salom	Táchira	7.6	-72.2	475	2966.1	724.6	60
29	San Cristóbal	Táchira	7.8	-72.2	898	1592.1	311.2	60
30	La Ceiba	Trujillo	9.6	-71.1	9	1701.1	496.8	60
31	La Pedregosa	Trujillo	9.7	-70.7	101	1719.3	649.3	70
32	Los Caracas	Vargas	10.6	-66.6	15	956.8	603.2	30
33	Urachiche	Yaracuy	10.2	-69.0	486	1396.7	561.1	55
34	Sierra Azul	Zulia	10.9	-72.3	80	1395.4	710.6	80
35	Catatumbo	Zulia	8.9	-72.2	13	2971.6	875.2	80

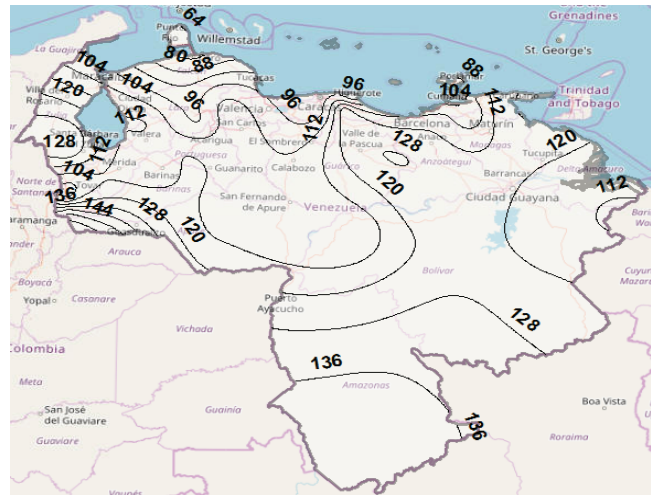
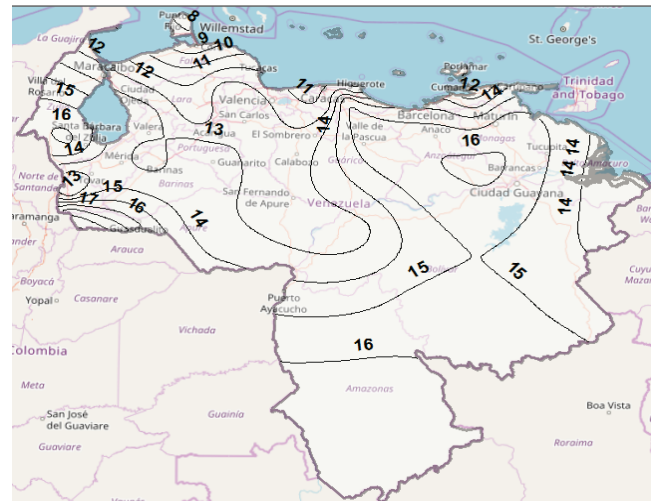
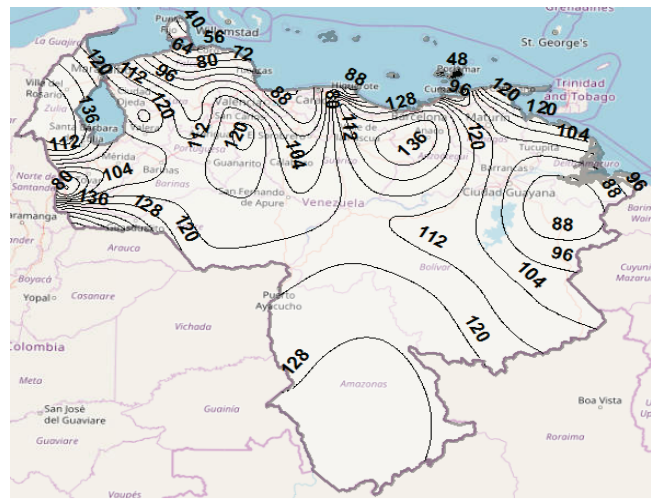
Source: The Authors.

Table 2.

Rainfall Rate for 0.01% and 0.5% of time.

Rice-Holmberg		Refined MM		ITU-U P.837-7	
0.01%	0.5%	0.01%	0.5%	0.01%	0.5%
132.2	13.2	138.6	16.6	95.3	14.9
125.0	11.7	133.1	16.0	90.2	13.7
93.1	5.9	101.2	12.2	72.5	7.2
105.2	6.4	105.7	12.7	80.2	8.3
80.9	5.7	98.8	11.9	67.4	6.6
103.2	7.1	108.5	13.0	70.2	8.5
115.9	6.8	109.1	13.1	74.0	8.7
111.5	8.8	118.2	14.2	84.8	10.9
88.2	5.7	99.7	12.0	67.6	6.8
116.1	5.3	104.3	12.5	74.1	7.9
91.2	8.1	114.0	13.7	83.4	10.0
83.8	4.2	91.7	11.0	58.4	5.2
48.3	1.5	71.2	8.6	42.2	1.4
97.4	6.7	105.8	12.7	80.6	8.3
93.9	4.6	95.8	11.5	60.2	6.0
90.6	5.3	98.2	11.8	64.8	6.5
101.5	8.1	114.4	13.7	72.6	9.5
98.0	6.7	106.3	12.8	62.8	7.8
123.1	9.1	118.7	14.3	89.0	11.1
90.5	5.5	99.0	11.9	66.6	6.7
97.5	6.8	106.6	12.8	75.2	8.3
108.8	9.2	121.2	14.5	88.9	11.6
85.6	3.1	87.7	10.5	60.8	4.3
40.6	3.8	83.7	10.1	56.5	3.5
106.4	7.6	111.5	13.4	75.6	9.2
109.7	6.9	108.4	13.0	82.3	8.9
90.3	7.1	107.6	12.9	79.2	8.6
120.6	11.3	132.4	15.9	81.2	12.8
83.8	7.5	110.0	13.2	65.3	8.5
107.2	7.7	112.2	13.5	78.7	9.5
121.4	7.6	112.6	13.5	79.1	9.6
91.9	4.4	94.6	11.4	62.9	5.8
108.6	6.3	105.8	12.7	71.4	8.1
125.0	4.1	105.8	12.7	77.9	8.2
134.4	12.7	132.5	15.9	101.8	14.5

Source: The Authors.

Figure 1. Rain rate contour map using RMM model for  $p = 0.01\%$ .  
Source: The Authors.Figure 2. Rain rate contour map using RMM model for  $p = 0.5\%$ .  
Source: The Authors.Figure 3. Contour map for rain rate for  $p = 0.01\%$ , using RH model.  
Source: The Authors.

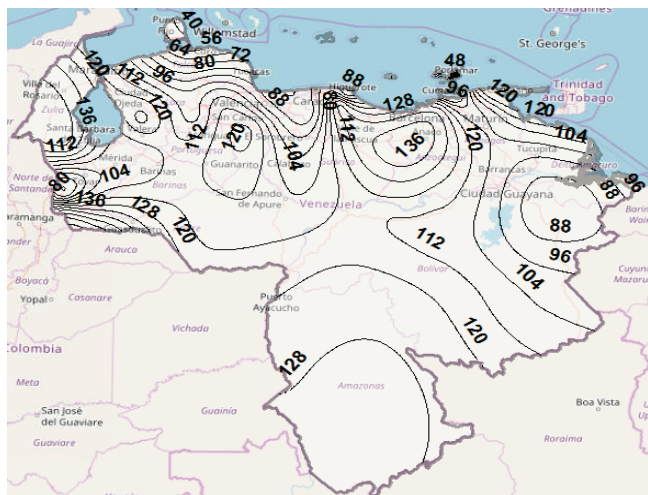


Figure 4. Contour map for rain rate for  $p = 0.01\%$ , using Recommendation ITU-R P.837-7.

Source: The Authors.

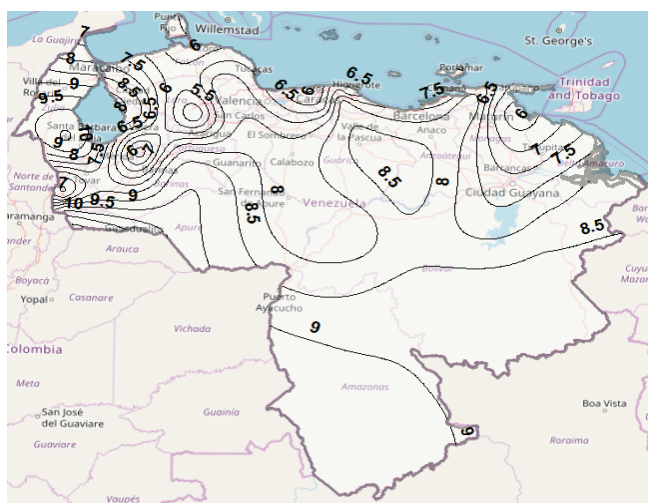


Figure 5. Contour map for rain attenuation for  $p = 0.5\%$ , using Recommendation ITU-R P.618-13 model, in Ku band.

Source: The Authors.

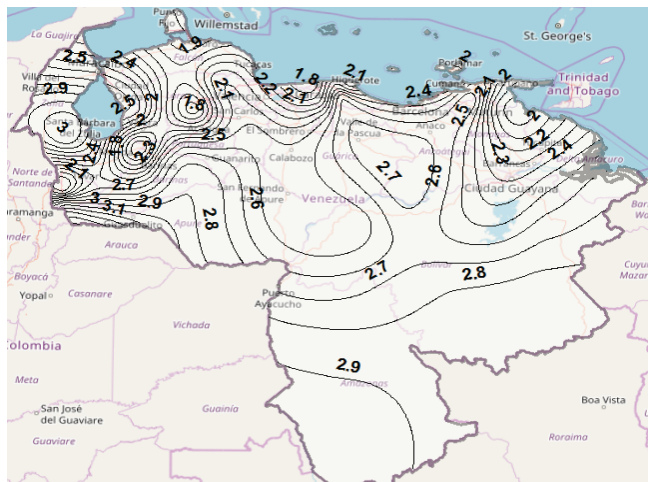


Figure 6. Contour map for rain attenuation for  $p = 0.5\%$ , using Recommendation ITU-R P.618-13 model, in Ka band.

Source: The Authors.

## 5. Rainfall attenuation contour maps in Venezuela

Using rain rate values estimated in section 4 and implementing Recommendation ITU-R P.618-13, Ramachandran-Kumar (RK), Yeo-Lee-Ong (YLO) and Rakshit-Adhikari-Maitra (RAM) models, rain attenuation contour maps in Venezuela were obtained. Attenuation was calculated for all meteorological stations of the Table 1, considering the downlink in Ku and Ka-bands (at 12 GHz and 20 GHz, respectively) with horizontal polarization.

As an example, based on rain rate results from Recommendation ITU-R P.837-7, Figs. 5 and 6 illustrate rain attenuation contour maps for Ku and Ka bands, respectively, when ITU-R P.618-13 model to attenuation prediction, with exceedance probability of 0.5%, is used. It can be seen that, as expected, rain attenuation is greater, in all locations, for the Ka-band. Furthermore, it is observed that the highest attenuations occur at northwestern zone (Zulia state), western region (Táchira state) and southern regions (Amazonas and Apure states), while the lowest values occur at western center zone (Lara state), Andes mountains area (Mérida state), northwestern region (Falcón state) and center region (Distrito Capital). Here it is important to emphasize that attenuation also depends on mean elevation above sea level of the earth station, elevation angle, among other factors.

Figs. 7 to 10 show rain attenuation contours maps for 0.01% of time, Ku band, using the four models considered in the study. The difference found in rain attenuation values expected for the country is observed. It is observed a difference in the rainfall attenuation values estimated for the country, by depending on the model used for the prediction. Again, it is important to point out that although the lack of measurements, this time, of rain attenuation in satellite links in Venezuela, it is not possible to determine which of the rainfall fade prediction models has the best performance, the results obtained are the preamble for the future real evaluation in the country of those models, or even other models not analyzed in this study, in order to reduce undersizing or oversizing of the system.

Finally, by comparing Figs. 5 and 7, an increase in rain attenuation could be observed when the percentage of time unavailability decreases. This is another expected aspect that should be considered by system designers.

## 6. Conclusions

In this paper, contour maps of 1-min rain rates and rain attenuation for exceedance probability of 0.01% and 0.5% have been shown in detail for the first time in Venezuela. This was achieved by using the Rice-Holmberg model, refined Moupfouma and Martin model and Recommendation ITU-R P.837-7 Annex 1 in order to convert monthly rain rate statistics in the country to rainfall rates with 1-min integration time and using the Recommendation ITU-R P.618-13, Ramachandran-Kumar, Yeo-Lee-Ong and Rakshit-Adhikari-Maitra models to estimate rain attenuation. The maps generated may be useful for preliminary “Simon Bolívar” satellite links planning in the country, because they may provide information quickly about the rain rate and rain attenuation levels.

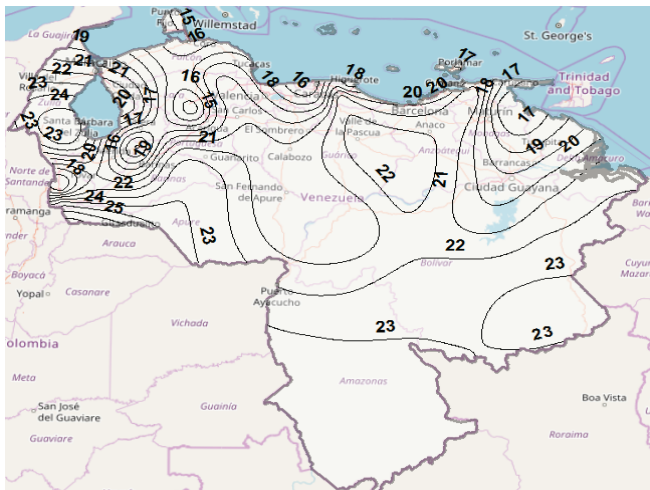


Figure 7. Rain attenuation contour map for  $p = 0.01\%$ , Ku band, using Recommendation ITU-R P.618-13.

Source: The Authors.

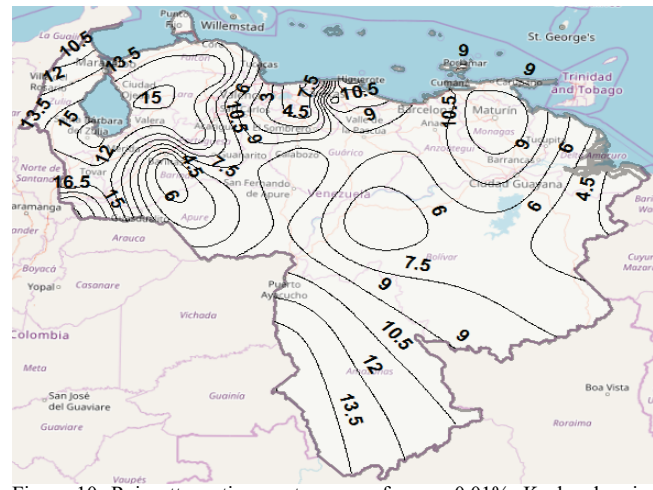


Figure 10. Rain attenuation contour map for  $p = 0.01\%$ , Ku band, using Recommendation ITU-R P.618-13.

Source: The Authors.

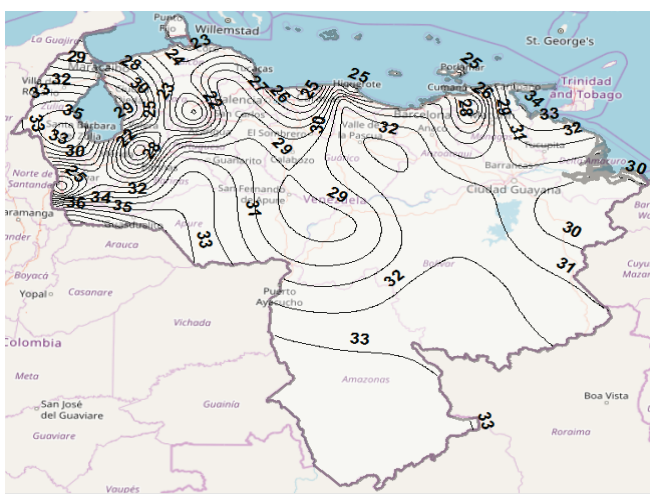


Figure 8. Rain attenuation contour map for  $p = 0.01\%$ , Ku band, using Ramachandran-Kumar model.

Source: The Authors.

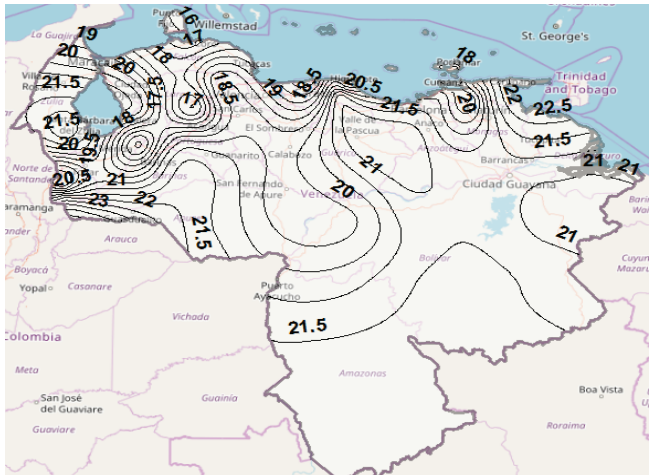


Figure 9. Rain attenuation contour map for  $p = 0.01\%$ , Ku band, using Yeo-Lee-Ong model.

Source: The Authors.

Nevertheless, measurements should be carried out in Venezuela in the future to evaluate performance of the models analyzed in this study, other models not included here, and also to develop rain rate prediction models and rain attenuation estimation models, adjusted to the climate characteristics of the country.

## 7. Appendix: rain attenuation calculation according to ITU-R P.618-13, RK, YLO and RAM models

The rain attenuation estimation in satellite communication systems is based on the link geometry illustrated in Fig. 11, whose parameters have been defined in section 3.

### 7.1. Recommendation ITU-R P.618-13

#### Step 1

$$h_R = h_0 + 0.36 \quad [\text{km}] \quad (12)$$

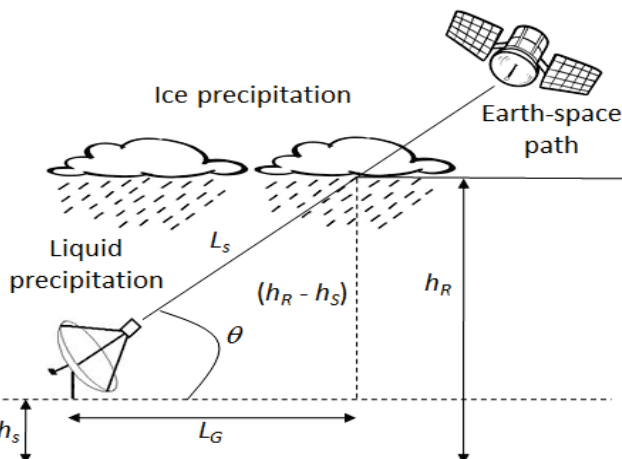


Figure 11. Schematic diagram of the Earth-space path.

Source: The Authors.

where  $h_0$  is the average height of the 0 °C isotherm. This height refers to the earth station site geographical coordinates and is given in Recommendation ITU-R P.839-4 [25].

**Step 2**

$$L_s = \begin{cases} \frac{2(h_R - h_s)}{\sqrt{\sin^2 \theta + \frac{2(h_R - h_s)}{R_E} + \sin \theta}}, & \text{for } \theta > 5^\circ \\ \frac{h_R - h_s}{\sin \theta}, & \text{for } \theta \geq 5^\circ \end{cases} \quad [\text{km}] \quad (13)$$

**Step 3**

$$L_G = L_s \cos \theta \quad [\text{km}] \quad (14)$$

**Step 4**

Obtain the rain rate  $R_{0.01}$ , exceeded during 0.01% of time in an average year, for a 1-min integration time. This parameter should better be obtained from measurements of the rainfall rate corresponding to the location of the earth station. However, in the absence of such an information, the rain rate Recommendation ITU-R P.837-7 [6] database can be used.

**Step 5**

$$\gamma_{0.01} = k R_{0.01}^\alpha \quad [\text{dB}/\text{km}] \quad (15)$$

where  $k$  and  $\alpha$  are the regression coefficients that depend on the operation frequency and wave polarization and are given by Recommendation ITU-R P.838-3 [26].

**Step 6**

$$r_{0.01} = \frac{1}{1 - 0.38(1 - e^{-2L_G}) + \sqrt{\frac{L_G \gamma_{0.01}}{f}}} \quad (16)$$

**Step 7**

$$\nu_{0.01} = \frac{1}{1 + \sqrt{\sin \theta} \left[ 31 \left( 1 - e^{-\frac{\theta}{1+\chi}} \right) \sqrt{\frac{L_R \gamma_{0.01}}{f}} - 0.45 \right]} \quad (17)$$

$$\chi = \begin{cases} 36 - |\varphi|, & \text{if } |\varphi| < 36^\circ \\ 0, & \text{Otherwise} \end{cases} \quad [\text{degrees}] \quad (18)$$

$$L_R = \begin{cases} \frac{r_{0.01} L_G}{\cos \theta}, & \text{for } \zeta > \theta \\ \frac{h_R - h_s}{\sin \theta}, & \text{Otherwise} \end{cases} \quad [\text{km}] \quad (19)$$

$$\zeta = \arctan \left( \frac{h_R - h_s}{r_{0.01} L_G} \right) \quad [\text{degrees}] \quad (20)$$

**Step 8**

Calculate the effective path length  $L_E$ , as follows

$$L_E = L_R \nu_{0.01} \quad [\text{km}] \quad (21)$$

**Step 9**

$$A_{0.01} = \gamma_{0.01} L_E \quad [\text{dB}] \quad (22)$$

**Step 10**

$$A_p = A_{0.01} \left( \frac{p}{0.01} \right)^{-0.655-0.033 \ln p + 0.045 \ln A_{0.01} + \beta (1-p) \sin \theta} \quad [\text{dB}] \quad (23)$$

$$\beta = \begin{cases} 0, & \text{if } p \geq 1\% \text{ or } |\varphi| \geq 36^\circ \\ -0.005(|\varphi| - 36), & \text{if } p < 1\% \text{ and } |\varphi| < 36^\circ \text{ and } \theta \geq 25^\circ \\ -0.005(|\varphi| - 36) + 1.8 - 4.25 \sin \theta, & \text{Otherwise} \end{cases} \quad (24)$$

## 7.2. Ramachandran-Kumar model

The first 4 steps of RK model are identical to those of Recommendation ITU-R P.618-13. Likewise, steps 5 to 7 also unlike that of model ITU-R, with the exception that  $\gamma_{0.01}$ ,  $r_{0.01}$  and  $\nu_{0.01}$ , change to  $\gamma_B$ ,  $r_B$  and  $\nu_B$ , where the subscript  $B$  refers to the breakpoint explained in section 3.

**Step 8**

$$L_E = L_R \nu_B \quad [\text{km}] \quad (25)$$

**Step 9**

$$A_B = \begin{cases} \gamma_B L_E C_f, & \text{if } 40^\circ \leq \theta \leq 60^\circ \\ \gamma_B L_E, & \text{Otherwise} \end{cases} \quad [\text{dB}] \quad (26)$$

$$C_f = -0.002 \theta^2 + 0.175 \theta - 2.3 \quad (27)$$

**Step 10**

Obtain estimated attenuation, in dB, to be exceeded for  $p(\%)$  of time an average year.

For  $p \leq 0.021$

$$A_p = A_B \left( \frac{p}{0.021} \right)^{-0.5[0.655+0.033 \ln p^2 - 0.03 \ln p - 0.045 \ln A_B - \beta (0.989-p) \sin \theta]} \quad (28)$$

For  $0.021 \leq p < 1$

$$A_p = A_B \left( \frac{p - 0.011}{0.021} \right)^{-0.655-0.033 \ln(p-0.011) + 0.045 \ln A_B + \beta (0.989-p) \sin \theta} \quad (29)$$

where the parameter  $\beta$  is given by Eq. (24).

## 7.3. Yeo-Lee-Ong model

The first 5 steps of the YLO model are the same as Recommendation ITU-R P.618-13.

**Step 6**

$$r = \frac{1}{\frac{0.3979}{\sin \theta} + 0.0021 R_{0.01} (H - h_s) - 0.0185 f + 0.2337} \quad (30)$$

**Step 7**

$$A_{0.01} = \gamma_{0.01} L_S r \quad [\text{dB}] \quad (31)$$

**Step 8**

$$A_p = A_{0.01} \left( \frac{p}{0.01} \right)^{-1.0063-0.0591 \ln p + 0.1317 \ln A_{0.01} + \beta (1-p) \sin \theta} \quad [\text{dB}] \quad (32)$$

$$\beta = \begin{cases} 0, & \text{if } p \geq 1\% \text{ or } |\varphi| \geq 36^\circ \\ -0.005(|\varphi| - 36), & \text{if } p < 1\% \text{ and } |\varphi| < 36^\circ \text{ and } \theta \geq 25^\circ \\ -0.005(|\varphi| - 36) + 1.7 - 7.85 \sin \theta, & \text{Otherwise} \end{cases} \quad (33)$$

#### 7.4. Rakshit-Adhikari-Maitra model

##### Step 1

In RAM model, rain height above the mean sea level is calculated as follows

$$H_r = h_R = \begin{cases} H_0, & \text{for } R_p \leq 10 \text{ mm/h} \\ H_0 + \log \frac{R_p}{10}, & \text{Otherwise} \end{cases} \quad [\text{km}] \quad (34)$$

where  $H_0$  is the same elevation above sea level of the earth station,  $h_s$ .

##### Step 2

In this case,  $L_s$  is given only by

$$L_s = \frac{H_r - H_0}{\sin \theta} \quad [\text{km}] \quad (35)$$

##### Step 3

$$\gamma_p = k R_p^\alpha \quad [\text{dB}/\text{km}] \quad (36)$$

##### Step 4

Calculate the attenuation to be exceeded for  $p(\%)$  of time an average year.

For  $R_p \leq 10 \text{ m/h}$

$$A_p = \gamma_p L_s \quad [\text{dB}] \quad (37)$$

For  $R_p \geq 10 \text{ m/h}$

$$A_p = \gamma_p \left[ \frac{1 - e^{-\left( \alpha \Gamma L_s \cos \theta \ln \frac{R_p}{10} \right)}}{\alpha \Gamma \cos \theta \ln \frac{R_p}{10}} \right] \quad [\text{dB}] \quad (38)$$

In Eq. (38), the rainfall decay parameter  $\Gamma$ , depends on rainfall rate  $R_p$  and is obtained from [5].

#### Acknowledgement

We are grateful to Instituto Nacional de Meteorología e Hidrología (INAMEH) from Venezuela for providing us with the rainfall data used in this research.

#### References

- [1] Pérez-García, N.P., et al., Fenómenos atmosféricos que afectan a las comunicaciones vía satélite, in Perez-García, N.A., Pinto-Mangones, A.D., Torres-Tovio, J.M. and Ramirez, E.J., Planificación y dimensionamiento de sistemas de comunicación vía satélite, Montería, Colombia, Sello Editorial Corporación Universidad del Sínú, 2018, pp. 36-71. ISBN: 978-958-8533-52-8
- [2] International Telecommunication Union – Radiocommunication, Recommendation P.618-13: propagation data and prediction methods required for the design of earth-space telecommunication systems, Geneva, Switzerland, 2017.
- [3] Ramachandran, V. and Kumar, V., Modified rain attenuation model for tropical regions for Ku-band signals. Int. J. Satell. Commun. Netw., 25(1), pp. 53-67, 2007. DOI: 10.1002/sat.846
- [4] Yeo, J.X., Lee, Y.H. and Ong, J.T., Rain attenuation prediction model for satellite communications in tropical regions. IEEE Trans. Antennas Propag., 62(11), pp. 5775-5781, 2014. DOI: 10.1109/TAP.2014.2356208
- [5] Rakshit, G., Adhikari, A. and Maitra A., Modelling of rain decay parameter for attenuation estimation at a tropical location. Adv. Space Res., 59(12), pp. 2901-2908, 2017. DOI: 10.1016/j.asr.2017.03.028
- [6] International Telecommunication Union – Radiocommunication, Recommendation P.837-7: Characteristics of precipitation for propagation modelling, Geneva, Switzerland, 2017.
- [7] Luini, L., Emiliani, L., Boulanger, X., Riva, C. and Jeannin N., Rainfall rate prediction for propagation applications: Model performance at regional level over Ireland. IEEE Trans. Antennas Propag., 65(11), pp. 6185-6189, 2017. DOI: 10.1109/TAP.2017.2754448
- [8] Rice, P.L. and Holmberg, N.R., Cumulative time statistics of surface-point rainfall rates. IEEE Trans. Commun., 21(10), pp. 1131-1136, Oct. 1973. DOI: 10.1109/TCOM.1973.1091546
- [9] Moupouma, F. and Martin L., Modelling of the rainfall rate cumulative distribution for the design of satellite and terrestrial communication systems. Int. J. Satell. Commun., 13(2), pp. 105-115, 1995. DOI: 10.1002/sat.4600130203
- [10] Rujano-Molina, L.M., Perez-Garcia, N.A. y Nariño-González T., Distribuciones acumulativas de la tasa de lluvias con tiempo de integración de 1-minuto en Venezuela. Ingeniería Al Día [Online], 3(1), pp. 24-44, 2017 [date of reference: April 10th, 2018]. Available at: <http://revista.unisini.edu.co/revista/index.php/>
- [11] Vieux, B.E., Distributed hydrologic modeling using GIS, 3rd ed. Netherlands: Springer, 2016, pp. 54-61. ISBN: 978-94-024-0930-7
- [12] Emiliani, L.D., Agudelo, J., Gutierrez, E. and Fradique-Mendez C., Development of rain-attenuation and rain-rate maps for satellite system design in the Ku and Ka bands in Colombia. IEEE Antennas Propag. Mag., 46(6), pp. 54-68, 2004. DOI: 10.1109/MAP.2004.1396736
- [13] Ojo, J.S., Ajewole, M.O. and Emiliani, L.D., One-minute rain-rate contour maps for microwave-communication-system planning in a tropical country: Nigeria. IEEE Antennas Propag. Mag., 51(5), pp. 82-88, 2009. DOI: 10.1109/MAP.2009.5432046
- [14] Ojo, J.S. and Owolawi, P.A., Development of one-minute rain-rate and rain-attenuation contour maps for satellite propagation system planning in a subtropical country: South Africa. Adv. Space Res., 54(8), pp. 1487-1501, 2014. DOI: 10.1016/j.asr.2014.06.028
- [15] Kestwal, M.C., Joshi, S. and Garia L.S., Prediction of rain attenuation and impact of rain in wave propagation at microwave frequency for tropical region (Uttarakhand, India). Int. J. Microw. Sci. Technol., 2014, (Article ID 958498), pp. 1-6. 2014. DOI: 10.1155/2014/958498
- [16] Imran, A.Z.M., Islam, M.T., Gafur, A. and Rabby, Y.W., Rain attenuation prediction analysis and contour map design over Bangladesh, Proceedings of the 18th International Conference on Computer and Information Technology (ICCIT 2015), Dhaka, Bangladesh, pp. 208-212, 2015. DOI: 10.1109/ICCIETechn.2015.7488069
- [17] Fialho, M.R.B., Silva, R.M.L., Pontes, M.S., Oliveira, C.H.R. and Gonsioroski, L.H., Mapas de contorno da taxa de chuva utilizando os históricos de dados acumulados de precipitação no Estado do Maranhão para modelagem de fenômenos radiometeorológicos, Anais do XXXIV Simpósio Brasileiro de Telecomunicações e Processamento de Sinais (SBrT 2016), Santarém, PA, Brasil, 2016, pp. 148-151.
- [18] Islam, M.R., Budalal, A.A.H., Habaebi, M.H., Badron, K. and Ismail, A.F., Performance analysis of rain attenuation on earth-to-satellite microwave links design in Libya, Proceedings of the 6th International Conference on Mechatronics (ICOM 2017), Kuala Lumpur, Malaysia, 2017, pp. 1-6.
- [19] Mandeep, J.S. and Hassan, S.I.S., Performances of existing rain rate models in equatorial region. J. Geophys. Res., 113(D11), pp. 1-7, 2008. DOI: 10.1029/2007JD009737
- [20] Chebil, J. and Rahman, T.A., Development of 1 min rain rate contour maps for microwave applications in Malaysia peninsula. Electron. Lett., 35(20), pp. 1172-1174, 1999. DOI: 10.1049/el:19991188

- [21] International Telecommunication Union - Radiocommunication Sector (ITU-R), P Series, Radiowave propagation, Recommendation P.1510-1: mean surface temperature, Geneva, Switzerland, 2017.
- [22] Stutzman, W.L. and Yon, K.M., A simple rain attenuation model for earth-space radio links operating at 10-35 GHz. Radio Sci., 21(1), pp. 65-72, 1986. DOI: 10.1029/RS021i001p00065
- [23] Instituto Nacional de Meteorología e Hidrología [Online]. [date of reference: March 31<sup>th</sup>, 2018]. Available at: <http://www.inameh.gob.ve/web/>
- [24] ArcGIS [Online]. [date of reference: June 23th, 2018]. Available at: <https://www.esri.com/es-es/arcgis/about-arcgis/overview>
- [25] International Telecommunication Union – Radiocommunication, Recommendation P.839-4: rain height model for prediction methods, Geneva, Switzerland, 2013.
- [26] International Telecommunication Union – Radiocommunication, Recommendation P.838-3: specific attenuation model for rain for use in prediction methods, Geneva, Switzerland, 2005.

**A.D. Pinto-Mangones**, is a BSc. in Systems Eng. from the Universidad del Sinú, Monteria, Colombia, in 2004. He received the MSc degree in Telematics and PhD. degree in Management Science and Technology, both from URBE, Maracaibo, Venezuela, in 2015 and 2016, respectively. Since 2009, Dr Pinto-Mangones has been a full professor at the Departamento de Ingeniería de Sistemas, Universidad del Sinú, Colombia.  
ORCID: 0000-0002-6792-8095

**N.A. Pérez-García**, is a BSc. in Electrical Eng. from the Universidad de Los Andes (ULA), Mérida, Venezuela, in 1992. He obtained MSc. and PhD. degrees in Electrical Engineering (Applied Electromagnetism area), from the Pontifícia Universidade Católica do Rio de Janeiro (PUC/Rio), Brasil, in 2000 and 2003, respectively. Since 1994, Dr. Pérez-García he is a full professor of ULA, Mérida, Venezuela.  
ORCID: 0000-0002-6163-933X

**J.M. Torres-Tovio**, is a BSc. in Informatics Eng. from the Universidad Católica del Norte, in Medellin, Colombia, in 2005. He received the PhD degree in Management of Science and Technology from URBE, Maracaibo, Venezuela, in 2015. Since 2015. Dr. Torres-Tovio has been a full professor at the Universidad del Sinú, Monteria, Colombia.  
ORCID: 0000-0002-9368-1436

**E.J. Ramírez**, is an Electrical Engineer from the Universidad de Los Andes (ULA), Merida, Venezuela, in 2003. Currently, he is a candidate for MSc (Telecommunications) and PhD (Applied Science) degrees at ULA.  
ORCID: 0000-0002-3728-4196

**S.O. Castaño-Rivera**, is a Systems Engineer and holds a MSc degree in Open Software from Universidad Autónoma de Bucaramanga, Colombia, in 2009. He is currently a professor in Universidad de Córdoba, Montería, Colombia.  
ORCID: 0000-0003-3302-3439

**J. Vélez-Zapata**, is an Electronic Engineer from Universidad de Antioquia, Colombia, and obtained PhD degree in Management of Science and Technology, at URBE, Maracaibo, Venezuela, in 2017. Currently, he is professor at Corporación Universidad de la Costa, Barranquilla, Colombia.  
ORCID: 0000-0002-0704-2292

**J.D. Ferreira-Rodríguez**, is a BSc in Electrical Eng. from the Universidad de Los Andes (ULA), Merida, Venezuela, in 1992, and PhD. from the University of Manchester, United Kingdom, in 2003. Since 1993, Dr. Ferreira-Rodríguez has been a full professor and a researcher at ULA. He is currently the research leader of the Institutional Projects called “Tren Electromagnético” (TELMAG) and Cohete Sonda, at ULA.  
ORCID: 0000-0001-6195-3516

**L.M. Rujano-Molina**, is a BSc. in Telecommunications Eng. from the UNEFA, Merida, Venezuela, in 2012. Obtained Lawyer degree and MSc degree in Telecommunications, from the Universidad de Los Andes (ULA), Merida, Venezuela, in 2016 and 2017, respectively.  
ORCID: 0000-0002-7015-6559



UNIVERSIDAD NACIONAL DE COLOMBIA

SEDE MEDELLÍN

FACULTAD DE MINAS

## Área Curricular de Medio Ambiente

### Oferta de Posgrados

Doctorado en Ingeniería - Recursos Hídricos

Maestría en Ingeniería - Recursos Hídricos

Maestría en Medio Ambiente y Desarrollo

Especialización en Aprovechamiento de

Recursos Hídricos

Especialización en Gestión Ambiental

Mayor información:

E-mail: acma\_med@unal.edu.co

Teléfono: (57-4) 425 5105